Multi-beam laser Doppler vibrometer for landmine detection

Vyacheslav Aranchuk
MetroLaser, Inc.
1 Coliseum Drive
University, Mississippi 38677
E-mail: aranchuk@metrolaserinc.com

Amit Lal, MEMBER SPIE
Cecil Hess
MetroLaser, Inc.
2572 White Road
Irvine, California 92614-6236

James M. Sabatier, MEMBER SPIE
University of Mississippi
1 Coliseum Drive
University, Mississippi 38677

Abstract. The method of buried landmine detection based on using elastic waves in the ground and a laser Doppler vibrometer (LDV) as a vibration sensor has shown excellent performance in field tests. To increase the speed of measurements, a multi-beam laser Doppler vibrometer (MB-LDV) was developed. The system is based on a heterodyne interferometer and is capable of simultaneously measuring the vibration of the ground at 16 points over a span of 1 m with a velocity resolution of less than 1 μm/s. Both digital in-phase and quadrature (I&Q) and analog phase-locked loop (PLL) demodulation have been used for signal processing. The MB-LDV can create a velocity image of the ground surface either in "stop-and-stare" mode or in a continuously scanning mode. The continuously scanning operation results in an increased velocity noise floor due to speckle noise. The speckle noise floor increases with the increase of the speed of the laser beam and can degrade the velocity image of a mine. To overcome the effects of speckle noise, the excitation source must provide a ground vibration velocity higher than the velocity noise floor of the vibrometer. The MB-LDV has been tested at landmine test lanes and shows the ability to detect buried landmine within a one-square-meter area in a time of less than 20 s. [DOI: 10.1117/1.2358975]

Subject terms: landmine detection; laser-acoustic sensing; seismic; acoustic; laser Doppler vibrometer (LDV).

Paper 050825R received Oct. 14, 2005; revised manuscript received Mar. 9, 2006; accepted for publication Mar. 27, 2006; published online Oct. 24, 2006. This paper is a revision of a paper presented at the SPIE Conference on Detection and Remediation Techniques for Mines and Minelike Targets X, Mar. 2005, Orlando, Florida. The paper presented there appears (unrefereed) in SPIE Proc. Vol. 5794.

1 Introduction

Techniques using low-frequency elastic waves in the ground have been successfully used for detecting buried landmines.[1–10] The method consists of excitation of the ground with elastic waves in the frequency range from about 50 Hz to 1000 Hz and using a vibration sensor to obtain a vibrational velocity map of the ground surface. The interaction of a buried landmine with the elastic waves causes the landmine to vibrate. The mine has a compliance higher than the compliance of soil and natural objects like rocks and roots, because it is a complex mechanical structure with moving parts such as a pressure plate, a trigger assembly, etc. Because of their complex structure, mines exhibit a resonance, while natural clutter objects do not. Due to the mechanical resonances of the mine and the higher mechanical compliance of the mine compared to the neighboring soil, the vibration amplitude of the ground surface above a mine is higher than the vibration amplitude of the surrounding area. A vibrometer measures the vibration of the ground in many points to create a vibrational map of the ground surface. A buried landmine can be detected by higher vibration amplitude of the surface area above the mine. Airborne sound created by loudspeakers, or seismic waves created by mechanical shakers, can be used to excite the ground vibration. A general schematic illustrating the principle of the method is shown in Fig. 1.

Using airborne sound to excite vibrations in the ground is based on the acoustic-to-seismic coupling phenomena.[1–4]

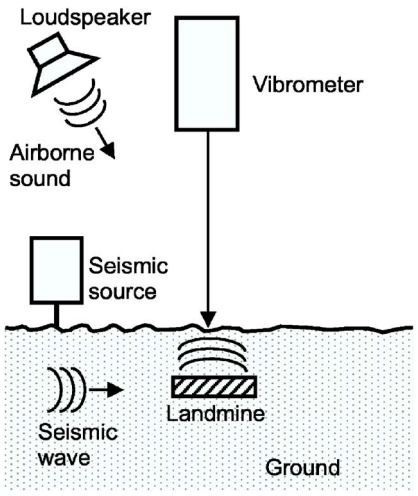

Fig. 1 Schematic illustrating the principle of acoustic landmine detection.

Airborne sound waves are incident onto the ground surface. When the sound waves penetrate the ground surface, they excite seismic motion. If a buried mine is present in the insonified area, the interaction of transmitted waves with the mine will change the ground vibration. The acoustic-to-seismic coupling-based technique was successfully used for detection of antitank and antipersonnel mines in field tests.[1–4,9,10] A single-beam scanning laser Doppler vibrometer (LDV) was used as a vibration sensor to create a velocity image of the ground surface. Field tests show that the acoustic-to-seismic coupling-based detection technique is able to detect mines with the probability of detection 95% or better and false alarm rate as low as 0.03 m^{-2}.

Elastic waves in the ground can also be excited with a surface-contacting seismic source.[5–8] The seismic source based on an electrodynamic transducer was designed to preferentially excite Rayleigh surface waves. The Rayleigh waves are an appropriate interrogation signal for the detection of buried landmines because they do not interrogate soil deeper than their wavelength and have relatively large surface displacement. The Rayleigh elastic wave propagates through the area of interest and causes surface displacement that can be measured with a noncontact vibration sensor. Waves interact with a mine, causing scattered waves and resonant oscillations of the mine and soil system. That results in an enhanced motion of the soil above the mine due to the compliance of the mine. Experiments show that both technique using airborne sound and technique using a surface-contacting seismic source can clearly differentiate mines from clutter such as roots, rocks, and sticks.[3,7,8,10]

Different sensors have been used for the vibration measurement of the ground surface.[11] The ground velocity can be sensed with contact sensors such as geophones and accelerometers, and with noncontact sensors such as microwave Doppler radar,[12] ultrasonic Doppler vibrometer,[12–15] Electronic Speckle-Pattern Interferometer,[11,16] and laser Doppler vibrometers.[1–4,9] LDVs have several advantages over other sensors, including high sensitivity, very good spatial resolution, and long working distances. In previous field experiments with buried antitank landmines,[3,10] LDV-based acoustic landmine detection has demonstrated a high probability of detection with very low false alarm rates.

The critical remaining issue in landmine detection is the speed of the measurement. The reliable detection of buried landmines requires a velocity image with relatively high spatial resolution. For example, the velocity image of an antitank mine typically contains from 16×16 to 22×22 points over a one-square-meter area,[3] and a velocity image of an antipersonnel mine might require 32×32 points.[4] Moreover, recent research has shown that higher spatial resolution can improve the detection of some antitank mines by obtaining velocity images of higher spatial vibration modes.[17,18] Vibration sensors currently used in landmine detection create the vibrational image of the target by sequential point-by-point measurements, which results in long measurement time. For example, using a single-beam scanning LDV, scanning a one-square-meter area with the required spatial resolution can take from 3 to 50 min. To reduce the measurement time, a continuously scanning single-beam LDV has been used.[19] Also a moving cart carrying 16 single-beam LDVs has been developed to reduce the measurement time of acoustic landmine detection.[20]

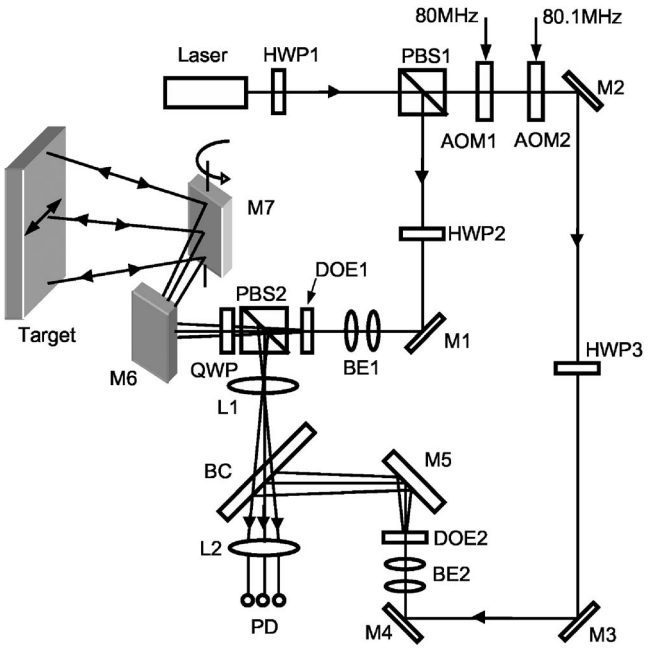

Fig. 2 Schematic of the scanning MB-LDV system. HWP1, 2, 3: half-wave plate; PBS1, 2: polarizing beamsplitter; AOM 1, 2: acousto-optical modulator; M1–M6: fold mirror; M 7: scanning mirror; DOE1, 2: diffractive optical element; QWP: quarter-wave plate; BE1, 2: beam expander; L1, 2: lens; BC: beam combiner; PD: fiber-coupled 16-photodiode array.

This paper describes a 16-beam Multi-Beam LDV (MB-LDV) recently developed for landmine detection, which provides parallel measurement of vibration in 16 points simultaneously. MB-LDV was successfully tested at US Army landmine test lanes,[21,22] and has shown a considerable reduction in the measurement time. The principles of operation of the MB-LDV, its operation in a continuously scanning mode, and experimental results of its application in the detection of buried landmines in field conditions are presented and discussed in the paper.

2 Schematics and Principles of Operation of the Multi-Beam Laser Doppler Vibrometer

A schematic of the MB-LDV is shown in Fig. 2. The system uses a single-mode, solid-state, continuous-wave, frequency-doubled (green) Nd:YAG laser with a wavelength of 532 nm and an output power of 200 mW. The optical configuration is based on a Mach-Zehnder interferometer with polarization separation of the beams. The polarizing beam splitting (PBS1) cube is used to divide the linearly polarized laser beam into an object beam and a reference beam. The *s*-polarized component of laser light is reflected by the beam splitter PBS1 to form an object beam, and the *p*-polarized component of the laser light passes through PBS1 and forms a reference beam. The relative ratio between the object and the reference beams can be adjusted with the half-wave plate HWP1 after the laser. The object beam passes through the half-wave plate HWP2, which changes its polarization from *s* to *p*. Then the object beam is directed to a diffractive optical element (DOE1), which divides it into 16 beams over an angle of 22 deg (for

simplicity, only three beams are shown in the figure). The beams pass through the polarizing beamsplitter (PBS2) and a quarter-wave plate (QWP) and are directed onto the target by using a fold mirror (M6) and a rotating mirror (M7). The quarter-wave plate changes the polarization of the object beam from linear to circular. The 16 beams illuminate a length of 1 m, with 63 mm separation between the beams. The scanning mirror allows the 16 beams to be scanned in the transverse direction. The light scattered from the target passes back through the quarter-wave plate, which now changes its polarization from circular to linear *s*-polarization, leading to a reflection at the polarizing beamsplitter PBS2. A collection lens (L1) then collimates the light from each of the 16 object beams. However, since the 16 object beams travel through the center of the collection lens, their path is unaltered and they retain the same angle originally imposed by the DOE.

The reference beam is frequency shifted by means of two acousto-optic modulators (AOMs). The two AOMs operate at 80.1 and 80.0 MHz, respectively, to produce a net frequency shift of 100 kHz. This frequency shift is obtained by using the +1-order diffracted beam from AOM1 as the input beam for AOM2; the −1-order diffracted beam of AOM2 has a 100-kHz frequency shift relative to the initial frequency of the laser radiation. The reference beam then passes through the half-wave plate HWP3, which changes its polarization from *p* to *s*, and is directed to another diffractive optical element (DOE2). DOE2 is identical to DOE1 and divides the reference beam into 16 beams with the same angular separation as the object beam. The 16 object beams and the 16 reference beams are spatially overlapped at the beam combiner (BC). A final lens (L2), placed one focal distance away from the collection lens makes the 16 object-reference beam pairs parallel and focuses them onto 16 individual fiber-coupled pin photodiodes, producing 16 heterodyne signals with a carrier frequency of 100 kHz.

The Doppler signal i_D at the output of each photodetector can be written:

$$i_D = kJ \cos[(\omega_R + \omega_D)t + \Phi], \tag{1}$$

where $J=2k(P_R P_S)^{1/2}$ is the amplitude of the Doppler signal $k=e\eta/h\nu$ is the sensitivity of the photodetector; P_R and P_S are the optical power of the reference beam and the scattered object light at the photodetector, respectively; e is the electron charge; η is the quantum yield; $h\nu$ is the photon energy; ω_R is the frequency shift of the reference light; ω_D is the Doppler shift of the scattered light due to vibration of the object; $\Phi=\Phi_R-\Phi_S$ is the phase of the Doppler signal; and Φ_R and Φ_S are the phase of the reference light and the scattered object light, respectively. The frequency shift of the reference light $f_D=100$ kHz defines the carrier frequency of the Doppler signal. The Doppler shift of the scattered light is related to the target velocity by;

$$\omega_D(t) = \frac{4\pi}{\lambda} V(t) \cos\beta, \tag{2}$$

where V is the vibration velocity of the target, $\lambda=532$ nm is the wavelength of the laser light, and β is the angle between the laser beam direction and the vibration velocity vector. The angle β varies from 0 deg to 11 deg for different beams of the MB-LDV, which results in slightly different velocity sensitivity for the different channels. These differences are compensated during the signal processing.

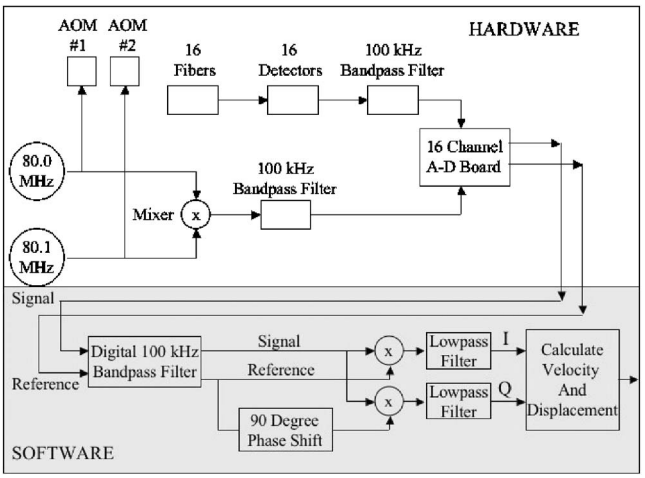

Fig. 3 Functional layout of the digital I&Q (in-phase and quadrature) demodulator.

The MB-LDV system used for landmine detection has the following basic specifications:

- Vibration velocity range: 1 μm/s to 5 mm/s
- Vibration frequency range: DC to 20 kHz
- Velocity resolution: 0.2 μm/s

Spatial resolution (beam separation): 63 mm

3 Doppler Signal Processing

The MB-LDV can use either an analog phase-locked loop (PLL) frequency demodulator or a digital in-phase and quadrature (I&Q) demodulator based on direct carrier sampling to obtain the vibration velocity information from the Doppler signal.

Figure 3 shows a functional layout of the digital I&Q demodulator. The system captures the reference and signal waveforms and uses these to calculate baseband I&Q signals, which can be processed to provide the target displacement or velocity. A pin diode photodetector at the output of each optical fiber converts each optical signal to an electric signal. The reference clock signal is obtained by sending the drive signals for the 80.0- and 80.1-MHz AOMs to a mixer. This produces outputs at the sum and difference frequencies; only the difference frequency is kept after passing through a 100-kHz bandpass filter. The reference clock and 16 FM signals (all with a carrier frequency of 100 kHz) are then simultaneously sampled with a 12-bit data acquisition board at sampling rates up to 600 kHz. After applying digital bandpass filters around 100 kHz, the reference clock is phase shifted by 90 deg in software. Then the reference and the phase-shifted reference clock are each multiplied with each beam signal, producing standard I (in-phase) and Q (quadrature) signals after lowpass filtering. From the I&Q waveforms, the displacement and velocity at each of the 16 beams can be calculated in software by using expressions:

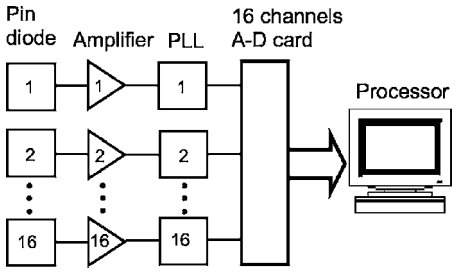

Fig. 4 Block diagram of the PLL-based signal processing.

$$X(t) = \frac{\lambda}{4\pi} \tan^{-1}\left[\frac{Q(t)}{I(t)}\right], \tag{3}$$

$$V(t) = \frac{\lambda}{4\pi}\left[\frac{I(t)\cdot Q'(t) - Q(t)\cdot I'(t)}{I^2(t) + Q^2(t)}\right], \tag{4}$$

where $X(t)$ and $V(t)$ are the vibration displacement and the vibration velocity, respectively, and $I'(t)$ and $Q'(t)$ are the time derivatives of in-phase I and quadrature Q components of the signal, respectively.

The functional layout of the analog PLL signal processing system is shown in Fig. 4. Signals from the 16 fiber coupled pin-photodiodes with a 100-kHz carrier frequency are amplified in the frequency band from 80 kHz to 120 kHz and then go to a 16-channel analog PLL frequency demodulator. The output of the PLL demodulator is proportional to the vibration velocity of the target. The PLL demodulator has a frequency range from DC to 4000 Hz. Each PLL output signal is then digitized with a 16-channel A-D card in a computer, and the velocity spectrum of each beam is calculated in software.

A two-dimensional velocity image of a target can be obtained by using either a "stop-and-stare" mode or a continuously scanning mode. In the stop-and-stare mode, the beams are moved a specified angle and stopped, the data are collected, and the beams are moved to the next location. In the continuously scanning mode, the beams are continuously scanned across the target at a specified speed, and the data are taken continuously during the scan. Figure 5 illustrates the signal processing for obtaining a velocity image of a target in the continuously scanning mode. In order to produce a velocity image, the time-domain velocity data for each beam is divided into time segments, typically of length from 0.1 s to 1 s.

Figure 5(a) shows an example of a 1-s time segment of the time-domain velocity signal for one of the beams passing over a mine. This time segment corresponds to the position of a scanning beam over a buried landmine. Over each time segment, the velocity versus time is Fourier analyzed to generate the velocity versus frequency data over each time segment for each beam. The frequency spectrum of the time segment of Fig. 5(a) is shown in Fig. 5(b). One can see that the mine shows a broad frequency response from about 100 Hz to 200 Hz.

When the velocity spectra over each time segment and each beam has been computed, a velocity image over the entire scanned area can be generated at any selected frequency band. The number of segments in the x direction

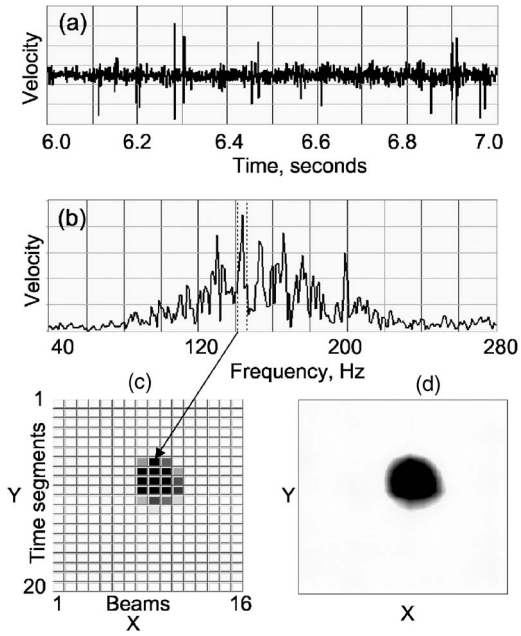

Fig. 5 Processing of the vibration velocity signals. (a) Time domain vibration velocity signal on the PLL output obtained for the 1-s time segment for one of the channels. (b) Frequency spectrum of that signal. (c) Segmented velocity image of the buried landmine in a specified frequency band (e.g., 140 to 145 Hz). The arrow shows the segment of the image whose velocity spectrum is shown in Fig. 5(b). (d) Smoothed velocity image of the buried landmine.

corresponds to the number of beams, while the number of segments in the y direction is defined by the time segment length and the duration of the entire scan. In the example shown in Fig. 5(c), 16 laser beams scanned the target of 1 m $\times$ 1 m from top to bottom (in the y direction) for a time of 20 s. The length of each time segment is 1 s, which corresponds to 5-cm spatial resolution. Therefore, the velocity image in this example contains 20×16 segments.

The modulus of the ground vibration velocity in each segment can be represented in different view styles: color map, gray scale map, isolines, or 3D image. The velocity image of the mine shown in Fig. 5(d) was obtained by applying a data smoothing algorithm to the segmented image. The described procedure can also be applied to the stop-and-stare mode of measurement. In the stop-and-stare mode, each time segment corresponds to a specific location of beams, while each time segment in the continuous scanning method is an average over a finite length.

4 Speckle Noise

Scanning a laser beam across a target introduces noise in the vibrometer output due to dynamic speckles. The LDV noise caused by dynamic speckles was first studied by Rothberg et al.[23] They showed that target motions such as in-plane motion, rotation, and tilt could increase the velocity noise floor due to speckle fluctuations. Coherent light scattering from an optically rough surface creates a speckle field. The statistical characteristics of laser speckles are well studied.[24] The phase of speckles is uniformly distributed in the range from $-\pi$ to π, and the intensity of speckles has a negative exponential probability distribution.

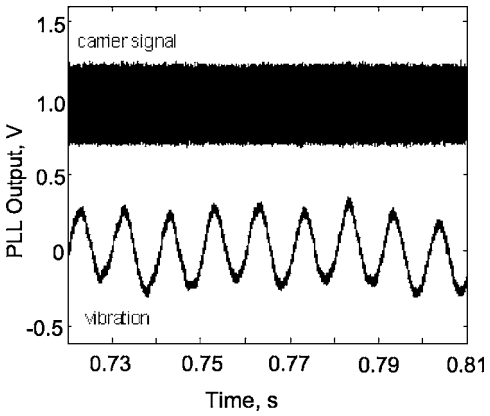

Fig. 6 Doppler signal and demodulated vibration velocity for a stationary beam.

When the laser beam moves across the target, the intensity and phase of speckles change in a random way. This results in random fluctuations of the amplitude and phase of the Doppler signal. Since the power P_S and phase Φ_S of scattered light on the photodetector are the power and phase of speckles, the Doppler signal expressed by Eq. (1) is a random signal with random amplitude and phase. For a laser beam stationary relative to the target, the amplitude and phase of the Doppler signal do not change with time. In this case, the Doppler signal is a space-random but not a time-random value. Figure 6 shows a 100-kHz carrier Doppler signal and a demodulated vibration velocity signal when the laser beam is stationary. The vibration is a sinusoidal signal with a frequency of 100 Hz. The amplitude of the carrier signal is a random value and depends on the intensity and phase of speckles on the photodetector area. The amplitude of the carrier signal changes with the position of the laser beam on the target but does not change with time.

When a beam moves across the target, the speckles at the photodetector vary, resulting in random variation of the Doppler signal amplitude and phase. The amplitude of the Doppler signal varies randomly and can occasionally drop down to a small value below the photodetector noise level. In that case, because of insufficient signal, the PLL can lose lock, which results in a spike in the PLL output. When the Doppler signal reappears, the PLL locks in again. Figure 7(a) shows the 100-kHz carrier Doppler signal and the demodulated velocity signal when the laser beam moves across the target. The demodulated velocity signal (PLL output) contains spikes caused by the speckle dropouts. Figure 7(b) shows an expanded view of the spike near 0.76 s and the corresponding drop in the carrier signal amplitude. The spikes in the demodulated signal have a broadband spectrum and increase the velocity noise floor of the vibrometer.

The phase fluctuation of the Doppler signal due to the motion of the laser beam is another effect that increases the velocity noise floor. It has been shown[23] that a change in the speckle pattern on the photodetector results in random fluctuations of the phase of the Doppler signal that increases the velocity noise floor of the vibrometer. The frequency f_C of the carrier Doppler signal at the LDV output is given by the time derivative of the argument in the cosine function in Eq. (1):

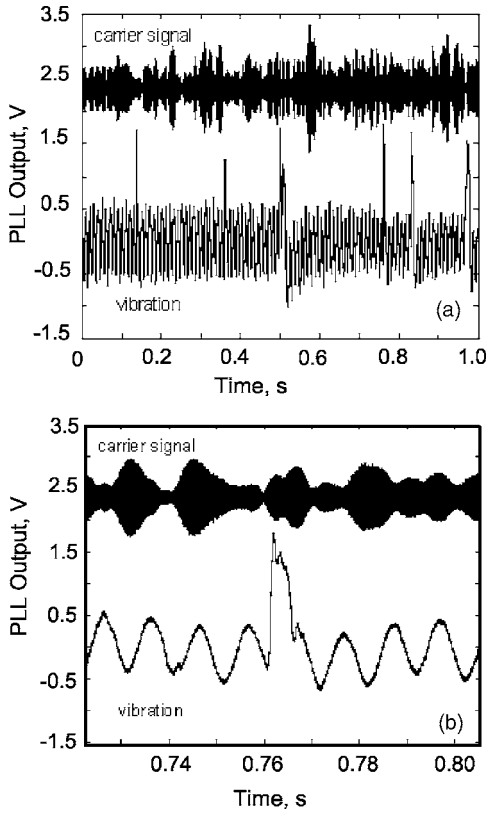

Fig. 7 (a) Doppler signal and demodulated vibration velocity for a moving beam. (b) Expanded view of the data between 0.72 and 0.80 s, showing the velocity spike and the corresponding drop in carrier signal amplitude.

$$f_C = f_R + f_D + \frac{1}{2\pi}\frac{\mathrm{d}\Phi(t)}{\mathrm{d}t}, \tag{5}$$

where f_R and f_D are the frequency shift of the reference light and the Doppler shift of the scattered light.

When the laser beam is stationary and a target exhibits only out-of-plane vibration, the speckles on the photodetector do not change with time and $d\Phi/dt=0$, making the frequency of the carrier Doppler signal equal to $f_C=f_R+f_D$.

When the speckles change due to a target motion such as rotation, in-plane vibration, angular vibration, or a beam moving across the target, the noise corresponding to the frequency content of $d\Phi/dt$ appears in the signal. It was shown[23,25] that when the speckle fluctuations are caused by a periodic motion of the target such as in-plane vibration, angular vibration, or rotation, the speckle motion is also periodic. As a result, the phase fluctuations of speckles will be pseudo-random with the same fundamental frequency as the frequency of the object vibration. In practice, the measured out-of-plane vibration has the same frequency as the angular and in-plane vibrations or is a multiple of the frequency of rotation of the object. That makes the fundamental frequency of speckle fluctuations the same as the fre-

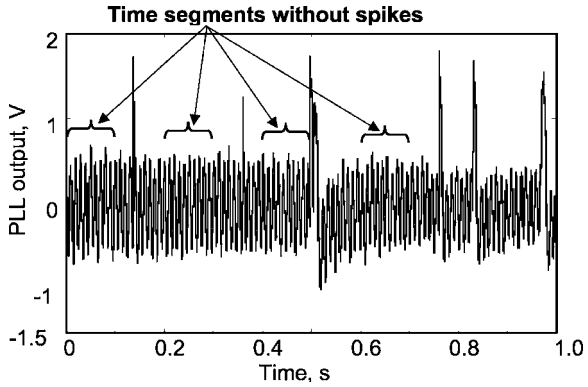

Fig. 8 Demodulated vibration velocity signal containing 0.1-s time segments with spikes and without spikes.

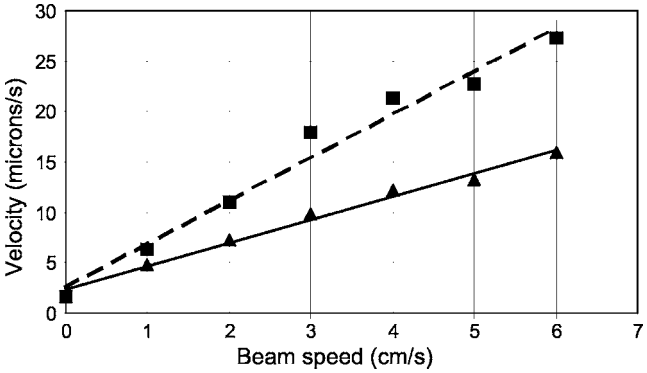

Fig. 9 Velocity noise floor versus scanning speed of the beam. The dashed line is the average noise floor over all time segments of length 0.1 s. The solid line is the average noise floor over time segments of 0.1 s without spikes.

quency of out-of-plane vibration. That signal content induced by phase fluctuations of speckles is indistinguishable from the out-of-plane vibration signal and was described as "pseudo-vibration."[23] Unlike pseudo-vibrations caused by a periodic motion of speckles, the phase fluctuations of speckles caused by a continuously scanning laser beam are not periodic by nature. As a result, these fluctuations produce random noise at the vibrometer output at a continuously scanning beam.

We have investigated experimentally how the velocity noise floor caused by a scanning laser beam depends on the speed of the beam and have studied the contribution of spikes and phase fluctuations of speckles into the speckle noise. A single beam from an LDV was used to scan a stationary target surface (white paper) at different speeds, and the velocity noise floor was calculated for each speed. In order to calculate the velocity noise floor caused by spikes and phase fluctuations of speckles separately, the demodulated signal was digitized and recorded. Then the signal was divided into time segments with a length of 0.1 s. Some of the time segments contain spikes caused by Doppler signal dropouts, while some of the segments are free of spikes. Figure 8 shows the demodulated signal containing time segments with spikes and without spikes. To find the velocity noise floor caused only by phase fluctuations of speckles, the average noise floor was calculated over the time segments without spikes. This noise floor is shown in Fig. 9 (solid line). The velocity noise floor was then calculated over all time segments, both with spikes and without spikes. The dashed line in Fig. 9 shows that noise floor. Figure 9 shows that both spikes and phase fluctuations of speckles contribute to the speckle noise. The noise caused only by the phase fluctuations of speckles and the noise caused by two effects, phase fluctuations and spikes, both increase with the speed of the scanning beams. In our experiments, the speed of the beam was limited to 6 cm/s, since there were no time segments of length 0.1 s without spikes at higher speeds. Figure 10 shows the dependence of the overall velocity noise floor of the PLL demodulated signal on the speed of the scanning beam higher than speed in Fig. 8. The velocity noise floor increases with the increase in the speed of the scanning beam.

5 Field Experiments

The MB-LDV has been successfully tested at US Army test lanes. The test was done in two different types of soil—sandy gravel and sandy clay. Real plastic and metal antitank mines and mine simulants have been buried in the test lanes for more than five years. The real mines contain the original explosive material, but the detonator has been removed for safety purposes. The mine simulants were filled with nonexplosive material with dielectric properties similar to explosive material. The mines were buried at different depths from 0 cm to 15 cm.

Both loudspeakers and mechanical shakers can be used to excite the ground. Loudspeakers are noncontact devices and provide a homogeneous sound pressure level over the ground surface due to the large wavelength of sound in the air. Mechanical shakers are contact devices and the mechanism of the vibration excitation of the ground is more complex than that of speakers. Different coupling of the mechanical energy into the soil due to the soil properties and the propagation of seismic waves through soil inhomogeneities result in unequal excitation of different parts of the ground area. Due to the different nature of the ground excitation, the frequency response of the ground to shakers and loudspeakers is different. The shakers have a limited frequency bandwidth; they produce high excitation at low frequencies but exhibit a high-frequency roll-off.[26] The loudspeakers excite ground vibrations over a wide bandwidth up to 1000 Hz. The shakers have an advantage over

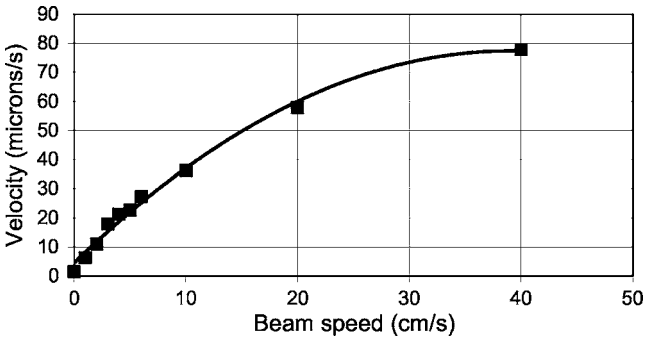

Fig. 10 Velocity noise floor versus the speed of a scanning beam.

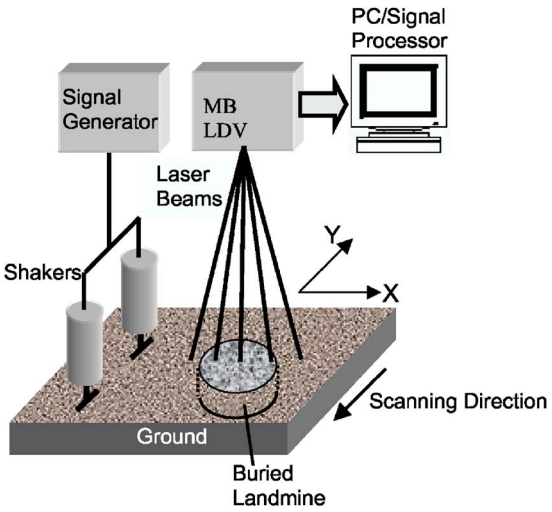

Fig. 11 Schematic of the experimental setup.

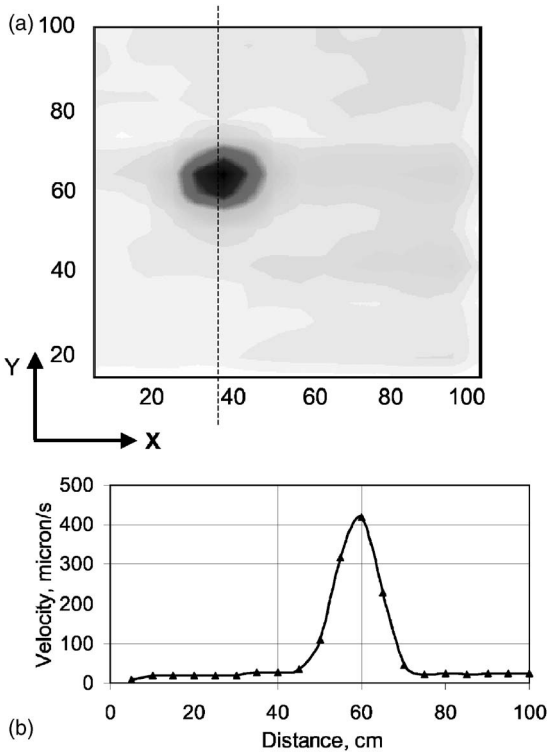

Fig. 12 Velocity image (a) and its spatial profile (b) measured along the dotted line of an antitank mine VS 1.6 buried 15 cm. deep in gravel. S/C=20.1.

the speakers in lower excitation of the vibrometer platform, since shakers radiate less sound in the air. Due to that advantage, mechanical shakers were used for the vibration excitation of the ground in the field experiments described here.

The layout of the experimental setup is shown in Fig. 11. The MB-LDV was mounted onto a moving platform at a height of 2.1 m above the ground. The laser beams scanned a 1 m$\times$1 m area above a buried antitank mine. The laser beams were positioned so that the mine was approximately in the middle of the scan. Two mechanical shakers were used to excite the vibration of the ground. The shakers were placed at a distance of 1 m from the first laser beam. Pseudo-random noise in the frequency range from 40 to 450 Hz was used as an excitation signal. The beams were oriented in the down-track direction, and were scanned in the across-track direction. The speed of beams on the ground in the continuously scanning mode could be set from 2 cm/s to 100 cm/s. The PLL demodulator was used to take data continuously during the time the beams scanned the ground. The PLL output signals were digitized with a 16-channel A-D card in a computer, and the data file was stored in the computer memory. The stored file was then processed with a custom MATLAB program to obtain a velocity image of the scanned area at a specified frequency band. Detection of a mine is based on the difference in the modulus of the vibration velocity between different areas of the ground, as well as the size and the shape of the high velocity area.[3] Figure 12 shows an example of the spatial profile of the velocity image of VS 1.6 antitank mine buried 15 cm deep in gravel soil. The detectability of the system can be measured by using the signal-to-clutter ratio (S/C) defined as the ratio of the velocity peak of the ground over the mine to the average velocity of the background area. The S/C ratio of the velocity image shown in Fig. 12 is 20.1. The speed of the scanning beams defines the spatial and frequency resolution of the velocity image of a scanned area. The speed of beams V_B is related to the spatial resolution S and the frequency resolution ΔF through the following expression[27]:

$$V_B = S \cdot \Delta F. \tag{6}$$

In many cases, a mine could be detected using a spatial resolution of 10 cm and a frequency resolution of 10 Hz. This makes the minimum time to scan one-square meter 1 s, taking into account that the time-domain signal corresponding to one-square-meter scan is divided into ten time segments of 0.1-s length. Each time segment corresponds to 10-cm spatial resolution and 10-Hz frequency resolution. Some mines require better spatial and frequency resolution to be detected. To provide better detection conditions, we scanned each area with a speed of 5 cm/s. The time of scanning a spot of one square meter was 20 s, which allowed us to obtain a velocity image with a spatial resolution of 5 cm along the scanning direction and a frequency resolution of 1 Hz. Figure 13 shows some velocity images and velocity profiles of different types of antitank mines buried at depths from 5 cm to 15 cm in sandy clay and sandy gravel obtained at the speed of beams 5 cm/s. The velocity profiles were calculated along a vertical line passing through the center of a mine image. The S/C ratio varied from 2 to more than 20 for antitank mines buried from 0 cm to 15 cm. The peak value of ground velocity over a mine varied from about 40 μm/s to 500 μm/s, depending on the type and the depth of the mine.

The tests performed show that the system was able to detect landmines buried in both types of soil equally well. About 95% of landmines under test (52 of 55) were detected.

Along with the restriction imposed by the required spatial and frequency resolution, the speed of a scanning beam

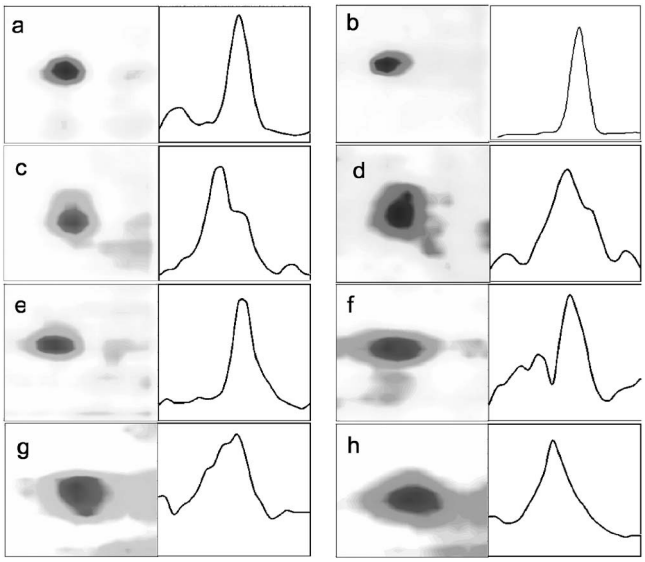

Fig. 13 Velocity images and velocity profiles of antitank mines buried in sandy clay [(a) to (d)] and in sandy gravel [(e) to (h)]. (a) Plastic VS2.2 mine at 7.5 cm, S/C=7.2. (b) Plastic VS1.6 mine at 15 cm, S/C=20.1. (c) Plastic TM62P mine at 5 cm, S/C=9.8. (d) Metal TM62M at 10 cm, S/C=5.3. (e) Plastic M15 mine at 7.5 cm, S/C=6.4. (f) Plastic M15 mine at 15 cm, S/C=3.2. (g) Plastic VS2.2 mine at 7.5 cm, S/C=2.6. (h) Plastic TM62P mine at 7.5 cm, S/C =4.0.

is also limited by speckle noise. In practice, the speckle noise defines the velocity noise floor of a continuously scanning LDV. The speckle noise increases with the increase in the speed of a scanning beam, as shown in Fig. 10. Increasing the speckle noise higher than the ground velocity of the background area lowers the S/C ratio of the velocity image. Figure 14 shows the S/C ratio of the velocity image of a buried antitank mine versus the speed of beams. The increase in the speed of beams from 2.5 cm/s to 5 cm/s [points (a) and (b) in the graph] results in an increase in the speckle noise but does not change the S/C ratio because the velocity of the background area remains higher than the velocity noise floor. When the speed of the beam increases to 10 cm/s [point (c) in the graph], the velocity noise floor becomes higher than the velocity of the background area, and the S/C ratio drops dramatically. Further increases in the speed of the beam result in a further increase in the velocity noise floor and a smooth decrease of the S/C ratio.

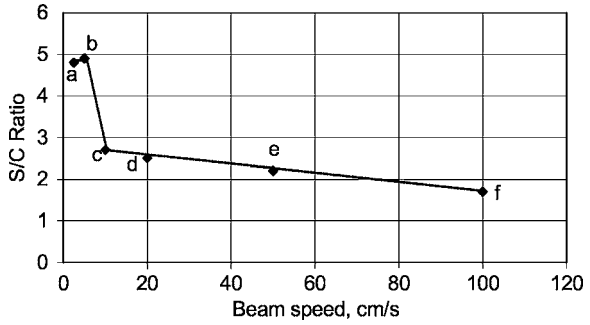

Fig. 14 Signal-to-clutter ratio of the velocity image of a buried antitank mine versus the speed of beams.

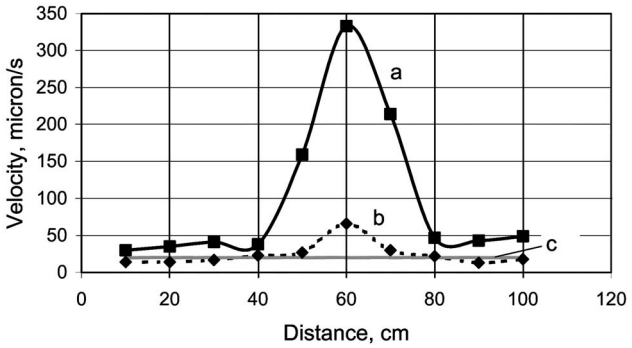

Fig. 15 Spatial profiles of the velocity image of an antitank mine buried 2.5 cm deep at different excitation levels. (a) Excitation level is 0 dB, S/C=8.2; (b) excitation level is –15 dB, S/C=3.5; (c) average velocity noise floor of the vibrometer.

To resolve the ground vibration velocity, the excitation level must provide a ground velocity higher than the velocity noise floor of the vibrometer. If the excitation is high enough for the velocity of the background area to stay higher than the velocity noise floor of the vibrometer, the S/C ratio does not change with the excitation level (assuming a linear response of the buried landmine and the ground). Figure 15 shows two velocity profiles of an antitank mine buried 2.5 cm deep obtained at different excitation levels. Curve (a) corresponds to the vibration excitation of the ground at which the ground vibration of the background area is higher than the velocity noise floor shown by curve (c). The S/C ratio at this excitation level is 8.2. Curve (b) shows the velocity profile of the mine at a 15-dB lower excitation level. At this excitation level, the ground velocity of the background area is lower than the velocity noise floor, so the measured velocity of the background area is actually the velocity noise caused by dynamic speckles. The S/C ratio of the velocity profile at the lower excitation level is only 3.5, in comparison to the 8.2 S/C ratio of curve (a).

6 Conclusions

The 16-beam multi-beam laser Doppler vibrometer (MB-LDV) for landmine detection can measure the vibration of the ground at 16 points simultaneously. It can measure ground vibration in both "stop-and-stare" mode and continuously scanning mode. Operation in a continuously scanning mode results in an increased velocity noise floor due to the amplitude and phase fluctuations of speckles. The velocity noise floor in a continuously scanning mode is affected by the speckle noise and increases with an increase in the speed of beams. Operation at higher scanning speed requires a higher excitation level to obtain a vibration velocity of the ground higher than the velocity noise floor of the vibrometer.

The MB-LDV has been successfully tested in field conditions. The velocity image of one square meter area of the ground can be obtained in a time from 1 s to 20 s, depending on the required spatial and frequency resolution. Field tests show that using the MB-LDV in a continuously scan-

ning mode with mechanical shakers for vibration excitation, a buried landmine can be reliably detected in a time of 20 s or less.

Acknowledgments

This material is based on work supported by US Army Research, Development, and Engineering Command, CERDEC Night Vision and Electronic Sensors Directorate, under Contract DAAB15-02-C-0024. The authors would like to express their thanks to Richard Burgett for his help in data acquisition and useful discussions and Ina Aranchuk for her contribution to the development of the signal processing software. The authors also wish to acknowledge contributions of Richard Mack in the experimental program.

References

1. J. M. Sabatier and N. Xiang, "Laser-doppler based acoustic-to-seismic detection of buried mines," *Proc. SPIE* **3710**, 215–222 (1999).
2. N. Xiang and J. M. Sabatier, "Land mine detection measurements using acoustic-to-seismic coupling," *Proc. SPIE* **4038**, 645–655 (2000).
3. J. M. Sabatier and N. Xiang, "An investigation of acoustic-to-seismic coupling to detect buried antitank mines," *IEEE Trans. Geosci. Remote Sens.* **39** (6), 1146–1154 (2001).
4. N. Xiang and J. M. Sabatier, "An experimental study on antipersonnel landmine detection using acoustic-to-seismic coupling," *J. Acoust. Soc. Am.* **113** (3), 1333–1341 (2003).
5. W. R. Scott Jr., J. S. Martin, and G. D. Larson, "Experimental model for a seismic landmine detection system," *IEEE Trans. Geosci. Remote Sens.* **39** (6), 1155–1164 (2001).
6. W. R. Scott Jr., G. D. Larson, J. S. Martin, and G. S. McCall II, "Field testing and development of a seismic landmine detection system," *Proc. SPIE* **5089**, 643–652 (2003).
7. W. R. Scott Jr. and J. S. Martin, "Experimental investigation of the acousto-electromagnetic sensor for locating land mines," *Proc. SPIE* **3710**, 204–214 (1999).
8. W. R. Scott Jr., S.-H. Lee, G. D. Larson, J. S. Martin, and G. S. McCall III, "Use of high-frequency seismic waves for the detection of buried land mines," *Proc. SPIE* **4394**, 543–552 (1999).
9. N. Xiang and J. M. Sabatier, "Laser Doppler vibrometer-based acoustic landmine detection using the fast M-sequence transform," *IEEE Trans. Geosci. Remote Sens.* **1**(4), 292–294 (2004).
10. E. M. Rosen, K. D. Sherbondy, and J. M. Sabatier, "Performance assessment of a blind test using the University of Mississippi's acoustic/seismic laser Doppler vibrometer (LDV) mine detection apparatus at A. P. Hill," *Proc. SPIE* **4038**, 656–666 (2000).
11. J. M. Sabatier, N. Xiang, A. G. Petculescu, V. Aranchuk, and M. Bradley, "Vibration sensors for buried landmine detection," in *Proc. Int. Conf. Requirements and Technologies for the Detection, Removal and Neutralization of Landmines and UXO*, Brussels, Belgium, pp. 483–488 (2003).
12. W. R. Scott Jr., C. Schroeder, and J. S. Martin, "An acousto-electromagnetic sensor for locating land mines," *Proc. SPIE* **3392**, 176–186 (1998).
13. A. G. Petculescu and J. M. Sabatier, "Doppler ultrasound techniques for landmine detection," *Proc. SPIE* **5415**, 30–34 (2004).
14. A. G. Petculescu and J. M. Sabatier, "Air-coupled ultrasonic sensing of grass-covered vibrating surfaces; qualitative comparisons with laser Doppler vibrometry," *J. Acoust. Soc. Am.* **115**(4), 1557–1564 (2004).
15. J. S. Martin, D. J. Fenneman, F. Codron, P. H. Rogers, W. R. ScottJr. , G. D. Larson, and G. S. McCall II, "Ultrasonic displacement sensor for the seismic detection of buried landmines," *Proc. SPIE* **4742**, 606–616 (2002).
16. J. M. Sabatier, V. Aranchuk, and W. C. K. Alberts II, "Rapid high-spatial-resolution imaging of buried landmines using ESPI," *Proc. SPIE* **5415**, 14–20 (2004).
17. J. M. Sabatier, R. Burget, and V. Aranchuk, "High frequency A/S coupling for AP buried landmine detection using laser Doppler vibrometers," *Proc. SPIE* **5415**, 35–41 (2004).
18. J. M. Sabatier, M. Corman, T. Witten, and D. Fenneman, "Detection of high impedance, weathered, buried landmines," Presented at the Conference "Detection and Remediation Technologies for Mines and Minelike Targets," SPIE Defense and Security Symposium, 29 March 2005, Orlando, FL.
19. N. Xiang and J. M. Sabatier, "Acoustic-to-seismic landmine detection using a continuously scanning laser Doppler vibrometer," *Proc. SPIE* **5089**, 591–595 (2003).
20. R. Burgett, M. Bradley, M. Duncan, J. Melton, A. Lal, V. Aranchuk, C. Hess, J. M. Sabatier, and N. Xiang, "Mobile mounted laser Doppler vibrometer array for acoustic landmine detection," *Proc. SPIE* **5089**, 665–672 (2003).
21. A. K. Lal, H. Zhang, V. Aranchuk, E. Hurtado, C. F. Hess, R. D. Burgett, and J. M. Sabatier, "Multiple-beam LDV system for buried landmine detection," *Proc. SPIE* **5089**, 579–590 (2003).
22. A. K. Lal, C. F. Hess, H. Zhang, E. Hurtado, V. Aranchuk, V. B. Markov, and W. T. Mayo, "Whole-field laser vibrometer for buried landmine detection," *Proc. SPIE* **4742**, 640–648 (2002).
23. S. G. Rothberg, J. F. Barker, and N. A. Halliwell, "Laser vibrometry: pseudo-vibrations," *J. Sound Vib.* **135** (3), 516–522 (1989).
24. J. W. Goodman, "Statistical properties of laser speckle patterns" in *Laser Speckle and Related Phenomena*, J. C. Dainty, Ed. (Springer, Berlin, 1975), pp. 9–75.
25. S. Rothberg and B. Halcon, "Laser vibrometry meets laser speckle," *Proc. SPIE* **5503**, 280–291 (2004).
26. V. Aranchuk, J. M. Sabatier, A. K. Lal, C. F. Hess, R. D. Burgett, and M. O'Neill, "Multi-beam laser Doppler vibrometry for acoustic landmine detection using airborne and mechanically coupled vibration," *Proc. SPIE* **5794**, 624–631 (2005).
27. N. Xiang and J. M. Sabatier, "Moving speed of linear acoustic landmine detection system," *Proc. SPIE* **5794**, 675–682 (2005).

Vyacheslav Aranchuk is a senior scientist at MetroLaser, Inc. He received his PhD in engineering from the Institute of Applied Physics of the National Academy of Sciences of Belarus in 1989. His research interests are in laser-based measurement technology with an emphasis on laser Doppler vibrometry and laser speckles. He is currently working on multi-beam and scanning laser Doppler vibrometers and their application.

Amit Lal is a senior scientist at MetroLaser, Inc. He received his BS in engineering physics from Princeton University in 1988 and his PhD in electrical engineering from UCLA in 1996. At MetroLaser, Dr. Lal is working on a variety of laser-based measurement systems, including laser Doppler vibrometers (LDVs), ultra-high-resolution interferometers, and digital holography applications. He is currently the leader of the Laser Vibrometer Group at MetroLaser, supervising the development, design, manufacture, and application of single-beam and multi-beam LDVs.

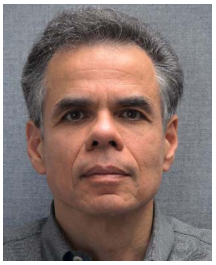

Cecil Hess is president and cofounder of MetroLaser, Inc., where he is responsible for the development of advanced technologies used in nondestructive testing, landmine detection, and gas turbine engine inspection. Under his supervision and guidance, new, advanced optical diagnostics techniques are developed, evaluated, and fielded. His experience includes developing particle sizing instruments, a multi-beam LDV system for whole-field vibration measurement, a Lidar CO_2 system for coherent Doppler measurements of sound and acoustic disturbances; managing several combustion diagnostics programs involving laser-induced fluorescence, Raman scattering, and resonant holography; and designing flow diagnostics instrumentation for engine test facilities. Hess received his PhD in mechanical engineering from UC Berkeley in 1978.

James M. Sabatier is a senior research scientist at the University of Mississippi's National Center for Physical Acoustics and a research professor of physics. He has served as principal investigator for several successful research projects for the Department of Defense and USDA. This research includes development of acoustic technologies for landmine detection, acoustic measurement of spatial and temporal physical properties of soils, and development of specialized loudspeakers. He holds a PhD in physics from the University of Mississippi (1984). He is a member of the Acoustical Society of America (ASA), the American Physical Society, SPIE, and the Soil Science Society of America, and he was elected a fellow of the ASA in 1992. His expertise is in the fields of physical acoustics, the interaction of sound with porous media, and outdoor sound propagation. He has published 42 papers in peer-reviewed journals and over 75 papers in proceedings and other journals.